

Graphical Abstract

Unleashing the Imagination of Text: A Novel Framework for Text-to-image Person Retrieval via Exploring the Power of Words

Delong Liu, Haiwen Li

Highlights

Unleashing the Imagination of Text: A Novel Framework for Text-to-image Person Retrieval via Exploring the Power of Words

Delong Liu, Haiwen Li

- Research highlight 1
- Research highlight 2

Unleashing the Imagination of Text: A Novel Framework for Text-to-image Person Retrieval via Exploring the Power of Words

Delong Liu^a, Haiwen Li^a

^a*Artificial Intelligence, Beijing University of Posts and Telecommunications, Beijing, 100876, China*

Abstract

The goal of Text-to-image person retrieval is to retrieve person images from a large gallery that match the given textual descriptions. The main challenge of this task lies in the significant differences in information representation between the visual and textual modalities. The textual modality conveys abstract and precise information through vocabulary and grammatical structures, while the visual modality conveys concrete and intuitive information through images. To fully leverage the expressive power of textual representations, it is essential to accurately map abstract textual descriptions to specific images.

To address this issue, we propose a novel framework to **Unleash the Imagination of Text (UIT)** in text-to-image person retrieval, aiming to fully explore the power of words in sentences. Specifically, the framework employs the pre-trained full CLIP model as a dual encoder for the images and texts, taking advantage of prior cross-modal alignment knowledge. The Text-guided Image Restoration auxiliary task is proposed with the aim of implicitly mapping abstract textual entities to specific image regions, facil-

itating alignment between textual and visual embeddings. Additionally, we introduce a cross-modal triplet loss tailored for handling hard samples, enhancing the model’s ability to distinguish minor differences.

To focus the model on the key components within sentences, we propose a novel text data augmentation technique. Our proposed methods achieve state-of-the-art results on three popular benchmark datasets, and the source code will be made publicly available shortly.

Keywords:

Text-to-image person retrieval, Cross-modal alignment, Text-guided image restoration, Cross-modal triplet loss

1. Introduction

Text-to-image person retrieval [34] refers to retrieving person images from a large gallery that match a given textual description. This task is significant for improving the accuracy and efficiency of image search and person recognition, and finds applications in fields such as social media analysis, image retrieval, and security monitoring. Conventional approaches typically [10, 27, 58, 63] combine deep learning and neural network techniques to align images and texts into a joint embedding space for image retrieval.

Text-to-image person retrieval is a challenging task. Unlike conventional text-to-image retrieval tasks [34, 42, 52], it involves retrieving person images from a large gallery that match a given textual description. As a result, the queried images do not differ in category but only in terms of details and attributes, which increases the difficulty of the task.

Moreover, there are significant differences in feature representation be-

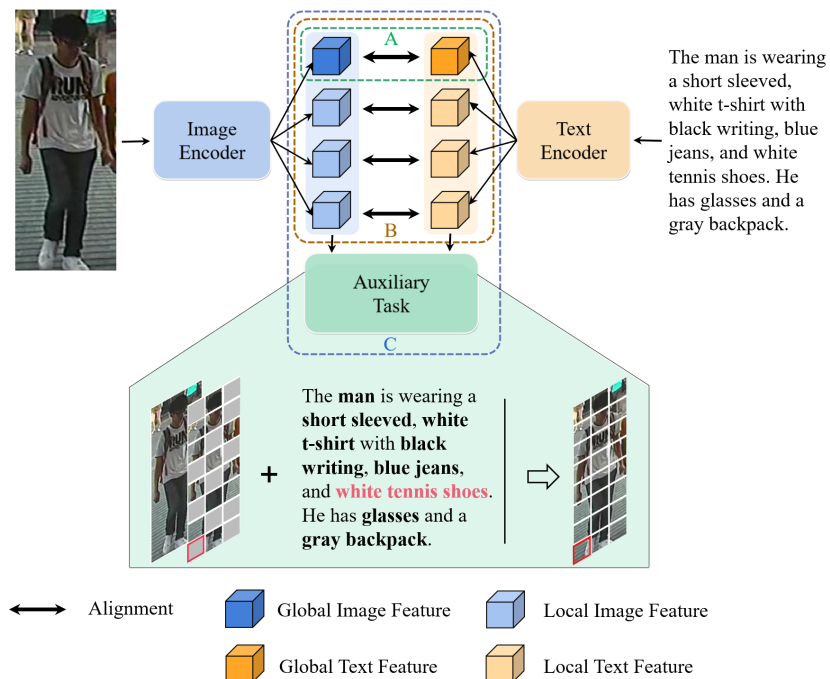


Figure 1: Illustration of the development of text-to-image person retrieval. The green dashed box (A) represents the early global-matching methods where global features are extracted separately from texts and images, followed by a matching and alignment process. The brown dashed box (B) represents subsequent methods that focus on local-matching. These methods explicitly extract local features from both images and texts while performing global and local feature matching and alignment. The blue dashed box (C) indicates more recent approaches that, in addition to feature alignment, leverage joint image-text auxiliary tasks to aid in implicit feature alignment.

tween visual and textual modalities. Visual modality focuses on conveying information through the intuitive traits, while textual modality conveys information through vocabulary and grammatical structures, possessing more abstract and flexible characteristics. The key to addressing this difference lies in adopting modal alignment methods that map visual and textual features

into a joint embedding space, facilitating effective alignment and matching between visual and textual modalities. Currently, prevalent approaches [13, 20, 59] utilize deep learning and neural network techniques to achieve visual and textual feature mapping, and compute the similarity between visual and textual embeddings for retrieval. However, different research periods have presented three directions in terms of minimizing the feature distance between positive sample pairs.

Early methods [20, 45, 64] (Figure 1A) tend to extract global features separately from images and texts, using matching losses for modal alignment. Although this approach has the lowest spatiotemporal complexity during model inference, its performance is generally lower due to the lack of effective interaction among features. Subsequent methods [10, 55, 63] (Figure 1B) establish explicit correspondences between local regions in images and phrases in texts that can significantly improve retrieval performance. However, such methods often require storing feature representations for local regions and phrases and matching them individually, which is inconvenient for large-scale practical scenarios. Recent methods [27, 49, 58] (Figure 1C) tend to incorporate cooperative auxiliary tasks between visual and textual embeddings on top of explicit feature matching, enabling implicit feature alignment. This approach typically does not increase the spatiotemporal complexity during inference while achieving higher performance. Therefore, the paper follows this framework for improvement.

This paper proposes a novel auxiliary task, namely Text-guided Image Restoration (TIR), aimed at better assisting the alignment of visual and textual embeddings, thereby achieving improved retrieval performance. As

shown in Figure 1, specifically, we introduce a decoder that leverages self-attention [53] mechanisms to jointly incorporate text and image information, with the objective of filling in randomly masked image patches. Taking the masked patch enclosed in the red box as an example (Figure 1), to effectively restore the missing patch, we generate restoration cues from the image information and utilize the phrase "white tennis shoes" to provide a qualitative description that guides the image restoration, aiming to restore the missing patch in a manner that closely resembles the original appearance. As multiple masked patches are restored, fine-grained correspondences between patches in images and phrases in sentences can be implicitly established, enhancing the accuracy of text-to-image person retrieval. Masked Image Modeling [24] (MIM) has been widely applied in visual pre-training [6, 19, 22] and has demonstrated remarkable effectiveness. In this paper, we demonstrate for the first time the robust effectiveness of MIM in downstream fine-tuning tasks across modalities.

To effectively supervise and guide image-text matching, the widely applied loss function is Cross-Modal Projection Matching (CMPM) loss [63], which maximizes the utilization of positive and negative sample pairs within the same mini-batch and exhibits strong stability. However, this loss function does not handle hard negative samples, making it difficult for the model to focus on these challenging samples during the update process. Recent research has introduced an image-text similarity distribution matching (SDM) loss [27], which successfully alleviates this issue by introducing a temperature coefficient. Based on SDM loss, we propose the Cross-Modal Triplet (CMT) loss, which focuses on the most challenging negative samples in a

mini-batch to enhance the model’s discriminative ability towards minor differences. Additionally, previous studies on person re-identification [25, 41, 54] have demonstrated the significance of color and texture information in distinguishing different identifications. Therefore, we propose a novel textual data augmentation method that randomly preserves attribute vocabulary in sentences to remind the model of the important components within the sentences.

Previous studies [27, 59] have shown that transferring knowledge directly from pretrained models like CLIP [44] can be a promising choice for image and text encoders. Our model architecture and training parameters for image and text encoders are directly inherited from the original CLIP. Specifically, compared to recent approaches [10, 48, 59], our proposed UIT computes the similarity score for global image-text pairs only once during inference, resulting in the lowest spatiotemporal complexity. The main contributions of our work can be summarized as follows:

1. Our proposed UIT effectively establishes the correspondences between body parts and textual entities by incorporating the Text-guided Image Restoration auxiliary task, implicitly enhancing the alignment of global features. This approach achieves remarkable results without additional supervision or inference costs.
2. We introduce the Cross-Modal Triplet loss to supervise the model in learning the slight differences between hard positive and negative sample pairs, thus improving its discriminative ability.
3. We propose a novel text augmentation method that randomly erases non-essential components in sentences, aiding the network in identify-

ing the key phrases.

4. Extensive experiments demonstrate that our UIT outperforms state-of-the-art techniques on three public benchmark datasets, i.e., CUHK-PEDES [40], ICFG-PEDES[13], and RSTPReid [65], showcasing its superior performance.

2. Related work

2.1. Text-to-image Person Retrieval

Text-to-image Person Retrieval [40] (TIPR) is a challenging cross-modal task that aims to align image and text features effectively in a joint embedding space for effective retrieval. In this field, a series of high-performance methods [10, 27, 59] have been proposed, which can be categorized into two main types, i.e., global matching and local matching. Global matching methods [4, 20, 27, 55] primarily focus on learning the overall similarity between images and textual descriptions. Early methods [4, 39, 40] utilized network architectures such as VGG [50] and LSTM [18] to learn representations for images and texts, aligning them through matching loss. With the introduction of models like ResNet [21] and Transformer [53], subsequent research improved the backbone networks for feature extraction, such as ResNet50/101 and BERT [12], and designed new cross-modal matching loss functions to align global image and text features in the joint embedding space. Local matching methods [10, 48, 55, 56, 59] aim to overcome the limitations of global matching methods by enhancing local alignment through extra modules [10, 56] or multi-task learning strategies [48, 60], such as human attribute recognition and body pose information. Some methods [10, 48, 60]

utilize multi-branches or attention mechanisms to learn local features related to body parts, color information, and textual entities to achieve local alignment. These methods outperform using global features alone in retrieval performance but also introduce additional computational complexity.

In addition to the explicit feature matching methods mentioned above, recent research [27, 49, 58] has explored the utilization of auxiliary tasks to implicitly assist feature alignment. These auxiliary tasks typically appear only during network training and do not increase additional inference costs while effectively improving network performance. Wu et al. [58] proposed the text-guided image coloring and Masked Language Modeling [12] (MLM) as auxiliary tasks, achieving impressive results. Subsequently, Jiang et al. [27] demonstrated the effectiveness of the MLM auxiliary task in their own research.

Previous methods [16, 38, 49] often initialized network parameters with pretrained models from a single modality, overlooking the correspondences between cross-modal information. In recent years, the rise of vision-language pretrained models [5, 35, 36, 37, 44], such as CLIP [44], has garnered attention from researchers. Some works [20, 27, 59] attempted to apply the CLIP model to the TIPR task, leveraging transfer learning to apply the knowledge from CLIP to this task and achieving excellent results. The latest research [27] has found that the pre-trained full CLIP model can be directly applied to text-to-image person retrieval and achieves remarkable performance when directly fine-tuned. Therefore, this paper adopts the pre-trained full CLIP model as encoder and fine-tunes it with relevant supervision.

2.2. Vision-Language Pre-training

The "pre-training and fine-tuning" [2, 8, 23, 36] paradigm is one of the most important paradigms driving the development of artificial intelligence. The basic process of this paradigm involves initializing the model parameters with a pre-trained model on a large-scale dataset [3, 32, 33, 43, 46] and then fine-tuning the model on various downstream tasks to achieve better performance leveraging the pre-trained model's prior knowledge. Vision-language pre-training [11, 36, 44, 62] (VLP) is a typical example of this paradigm in cross-modal tasks and has made significant progress. VLP aims to learn the semantic correspondences between visual and textual entities by pre-training on a large-scale dataset [3, 32, 43, 46] of image-text pairs. Inspired by the success of single-modality pre-training methods like BERT[12] and ViT [14], existing work on VLP is mainly based on Transformer [53] models. These models utilize a series of carefully designed pre-training tasks, such as image-text contrastive learning [35, 44, 62], masked language modeling [37, 62] and image caption generation [11, 37], to learn rich and context-aware feature representations with diverse semantic information. These feature representations not only capture the close relationship between visual and textual modalities but also effectively model complex visual and textual interactions, providing comprehensive, accurate, and robust cross-modal representations. Strong results have been achieved on downstream tasks such as image captioning [7], image-text retrieval [31], and visual question answering [1] by leveraging the powerful representational ability. VLP models can be divided into single-stream and dual-stream frameworks. Single-stream models [9, 29, 51] consist of a single Transformer encoder, resulting in fewer pa-

rameters. However, when handling cross-modal retrieval tasks, as the model needs to concatenate the textual and visual features as input, it becomes challenging to apply these models in practical scenarios as they require separate computations for each image-text pair during inference. On the other hand, dual-stream models [15, 26, 44] are well-suited for retrieval tasks as they only require one-time encoding of image and text features during inference. However, they may lack the modeling capacity to capture complex interactions between visual and textual modalities in other vision-language understanding tasks.

In summary, VLP is an important research direction that leverages large-scale datasets of image-text pairs for pre-training to learn the semantic correspondences between visual and textual entities. It has brought significant performance improvements to various downstream cross-modal tasks. We look forward to further utilizing the rich multimodal knowledge obtained from VLP models to advance the development of the TIPR task.

3. Method

The UIT framework is illustrated in Figure 2. There are two types of image inputs: complete images and images with randomly masked image patches. The text input has only one type, but there is a probability of retaining only the key components of the sentences. The network minimizes the feature distance between positive pairs through three representation learning branches and four types of loss functions. The identity(ID) loss [64] is used to aggregate feature representations of the same identity, while the SDM [27] loss and CMT loss are used to align the image and text features. The

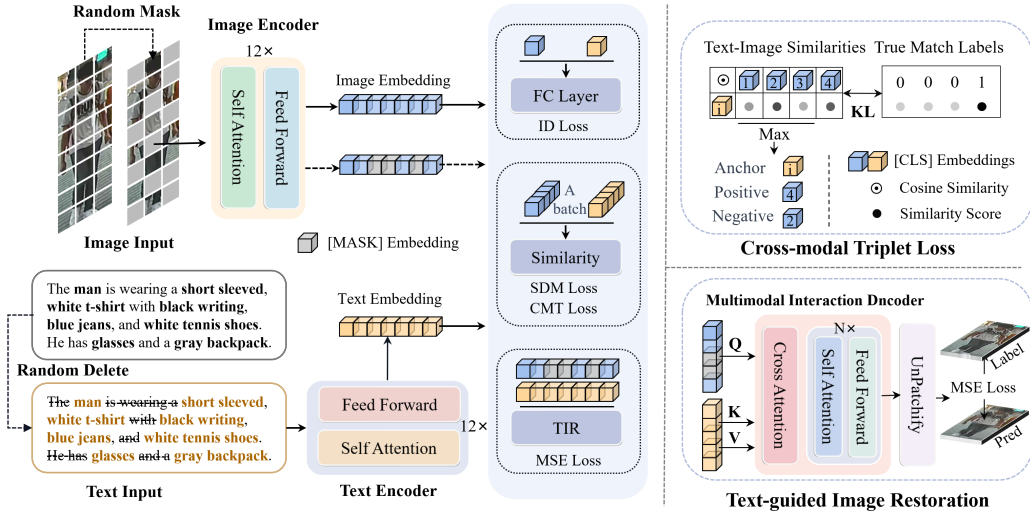


Figure 2: Overview of the proposed UIT framework. It consists of two feature encoders and one cross-modal feature decoder.

TIR module aims to establish fine-grained correspondences between image patches and phrases implicitly using the MSE loss. UIT aggregates the three branches for end-to-end training. During the inference stage, the network retains only the dual-encoder structure, thus computing the global image-text similarity score only once, resulting in high computational efficiency. Detailed description of each component will be provided in subsequent sections.

3.1. Image Encoder and Text Encoder

Before the groundbreaking progress of VLP, previous Text-to-Image Person Retrieval approaches typically relied on models pre-trained on a single modality for both images and texts. With the emergence of cross-modal pre-training models such as CLIP, some researchers have achieved promising results by transferring CLIP to Text-to-Image Person Retrieval. Therefore, in this study, the pre-trained full CLIP model is directly employed to initial-

ize the dual encoders in UIT, leveraging the prior knowledge of cross-modal alignment.

3.1.1. Image Encoder

Given an input image $I \in \mathbb{R}^{H \times W \times 3}$, the pre-trained CLIP ViT model is employed as the image encoder to obtain the embedded representation of the image. Firstly, the image I is divided into a series of equally-sized and non-overlapping patches, resulting in a total of $N^v = \frac{H \times W}{P^2}$ patches, where P represents the size of each patch. Subsequently, these patches are mapped to one-dimensional tokens through a trainable linear projection. To model the global information of these tokens and consider the correlation between patches, an additional [CLS] token is added, and positional information is introduced. Next, these tokens are inputted into a model with L_v -layer Transformer blocks to obtain the feature outputs $\{f_{\text{cls}}^v, f_1^v, \dots, f_N^v\}$, where f_{cls}^v represents the global feature, referred to as f^v in the subsequent context. This global representation can be used for image-text matching and related tasks.

3.1.2. Text Encoder

For the input text T , the pre-trained CLIP text encoder, which is an improved Transformer model [44], is utilized to extract text representations. Firstly, the input text description is tokenized using the Byte Pair Encoding [47] (BPE) with lowercase. To model the internal correlation of the text, special markers [SOS] and [EOS] are added to the tokenized text sequence to represent the start and end of the sequence, respectively. Additionally, a special marker [CLS] is introduced, and positional information is incorporated

into the tokenized text sequence. Next, this sequence of text tokens is inputted into a L_t -layer Transformer model, utilizing self-attention mechanism to capture the correlation between each part of the sequence. As a result, we obtain the output of the text encoding: $\{f_{\text{sos}}^t, f_1^t, \dots, f_{\text{cls}}^t, f_{\text{eos}}^t\}$, where f_{cls}^t represents the global feature, denoted as f^t in the subsequent context.

3.2. Text-guided Image Restoration

For Text-to-image person retrieval [40], numerous research studies [10, 58] have demonstrated the crucial importance of leveraging fine-grained information and establishing fine-grained correspondences between image and text representations. To effectively minimize the pronounced modality gap between vision and language, it is crucial not only to explicitly align image and text features but also to identify a suitable auxiliary task that can assist in achieving fine-grained alignment of image-text features. Specifically, we employ MIM as the auxiliary task to implicitly explore the fine-grained correspondences between image and text features by maximizing the mutual information between them. This approach facilitates the learning of more discriminative global features.

3.2.1. Text-guided Image Restoration

The MIM task was initially proposed for vision pre-training, where it utilizes random masking of input image patches and direct reconstruction of masked image patches for training. The TIR auxiliary task, which we propose, is based on MIM and aims to maximize the mutual information between images and text by recovering the masked image patches using textual information. Similar to the optimization approach in the MIM task, we

design a lightweight cross-modal decoder and mask a substantial portion of the image to facilitate a more meaningful cross-modal auxiliary task.

3.2.2. Multimodal Interaction Decoder

To achieve sufficient interaction and maximize mutual information between visual and textual modalities, we design a lightweight multimodal interaction encoder to fuse image and text embeddings. Inspired by the cross-modal encoder design in IRRA [27], our Multimodal Interaction Decoder (Figure 2) consists of a multi-head cross-attention (MCA) layer and N layers of Transformer blocks, maximizing computational efficiency while ensuring sufficient feature interaction.

Given the input image v , we first divide the image v into a series of equally-sized and non-overlapping image patches. A random masking process is applied to mask a percentage p_v of the image patches, resulting in a total of $N_{mask}^v = \lfloor N_p \times p_v \rfloor$ masked patches. These masked image patches are replaced with a special token [MASK]. The masked image patches are denoted as \hat{v} and passed through the image encoder as described in Section 3.1. Then, the final hidden states of the dual encoders $\{h_i^t\}_{i=1}^L$ and $\{h_i^{\hat{v}}\}_{i=1}^{N^v}$ are jointly inputted into the multimodal interaction encoder, where L is the length of the input text. To maximize the mutual information between image and text and more effectively fuse textual and masked image representations, the masked image representations $\{h_i^{\hat{v}}\}_{i=1}^{N^v}$ are used as queries (\mathcal{Q}), the textual representations $\{h_i^t\}_{i=1}^L$ are used as keys (\mathcal{K}) and values (\mathcal{V}). The global interaction between text and masked image representations can be achieved as follows:

$$\{h_i^c\}_{i=1}^{N^v} = \text{Transformer}(MCA(LN(\mathcal{Q}, \mathcal{K}, \mathcal{V}))) \quad (1)$$

where $\{h_i^c\}_{i=1}^{N^v}$ represents the context representation of the fused text and masked image, $LN(\cdot)$ denotes layer normalization, and $MCA(\cdot)$ represents the multi-head cross-attention, which can be expressed as:

$$MCA(Q, K, V) = \text{softmax}\left(\frac{QK^\top}{\sqrt{d}}\right)V \quad (2)$$

where d is the embedding dimension of the masked tokens.

For each masked position $\{h_i^c\}_{i=1}^{N_{mask}^v}$, we use a single-layer fully connected network to predict each pixel value within each image patch, denoted as $Pred$. Let $Pred_i^j$ be the value of the j -th pixel in the i -th image patch. Consequently, the loss of the TIR module is defined as:

$$\mathcal{L}_{tir} = \frac{1}{N_{mask}^v} \sum_{i=1}^{N_{mask}^v} \sum_{j=1}^{P^2} (Pred_i^j - True_i^j)^2 \quad (3)$$

where P denotes the size of each image patch, and $True_i^j$ represents the ground truth value of the j -th pixel within the i -th masked image.

Using TIR as an auxiliary task, compared to using MLM, demonstrates significant advantages with a same depth of the Transformer network. The output dimension of the last fully connected layer in the TIR task is P^2 , while the MLM task requires accurate word predictions, resulting in the last fully connected layer having a parameter dimension equal to the length of the vocabulary [27], often in the order of tens of thousands. Subsequent experiments have demonstrated that the TIR task achieves superior performance with higher parameter efficiency.

3.3. Cross-modal Triplet Loss

To further enhance the modeling capability of the model for fine-grained features, a new loss function called Cross-modal Triplet loss is introduced.

The CMT loss selects the most challenging negative sample pairs from $B \times B$ image-text pairs for enhanced learning. This approach allows the model to focus on challenging samples, thereby improving its encoding ability to capture subtle differences.

Given a mini-batch of data containing B image-text pairs, we construct a set of image-text pairs $\{(f_i^v, f_j^t), y_{i,j}\}_{j=1}^B$ on the global representation f_i^v of each image, where $y_{i,j}$ is a binary label indicating whether (f_i^v, f_j^t) belongs to the same identity ($y_{i,j} = 1$) or not ($y_{i,j} = 0$). Let $\text{sim}(\mathbf{u}, \mathbf{v}) = \mathbf{u}^\top \mathbf{v} / \|\mathbf{u}\| \|\mathbf{v}\|$ be the cosine similarity. The probability of a correct match can be calculated using the softmax function as follows:

$$p_{i,j} = \frac{\exp(\text{sim}(f_i^v, f_j^t) / \tau)}{\sum_{k=1}^B \exp(\text{sim}(f_i^v, f_k^t) / \tau)} \quad (4)$$

where τ is a temperature hyperparameter that controls the peakiness of the probability distribution. The matching probability $p_{i,j}$ can be seen as the proportion of the cosine similarity score between f_i^v and f_j^t and the sum of cosine similarity scores between f_i^v and $\{f_j^t\}_{j=1}^B$ in the mini-batch. For each image representation f_i^v , we can select the weakest positive sample corresponding to it in the same mini-batch as $p_i^t = \min \{f_j^t, y_{i,j} = 1\}_{j=1}^B$, and the most difficult negative sample as $n_i^t = \max \{f_j^t, y_{i,j} = 0\}_{j=1}^B$. Thus, the CMT loss from image to text in each mini-batch is calculated as:

$$\mathcal{L}_{i2t} = \frac{1}{B} \sum_{i=1}^B [\text{sim}(f_i^v, p_i^t) - \text{sim}(f_i^v, n_i^t) + \alpha]_+ \quad (5)$$

where $\text{sim}(\cdot, \cdot)$ denotes the cosine similarity, α is a hyperparameter, and $[x]_+$ denotes the positive value operation, i.e., $[x]_+ = \max(0, x)$.

Similarly, the CMT loss \mathcal{L}_{t2i} from text to image can be obtained by exchanging f^v and f^t in the above formulas. The bidirectional CMT loss is

computed as:

$$\mathcal{L}_{cmt} = \mathcal{L}_{i2t} + \mathcal{L}_{t2i} \quad (6)$$

To further improve the learning of global representations for images and text in the joint embedding space, we employ an ID loss [64] and an SDM [27] loss to explicitly supervise the feature alignment between images and text. The ID loss is a classification loss used to categorize the embedding vectors of images or text into different identity classes for supervised training. By introducing the ID loss, we can bring closer the feature representations belonging to the same identity within the same modality, thus promoting the learning and alignment of common features between images and text. The SDM loss utilizes KL divergence to simultaneously supervise the embedding of image-text pairs in the same mini-batch, aiming to decrease the distance between positive pairs and increase the distance between negative pairs in the joint embedding space, thereby associating the feature representations of different modalities.

In conclusion, UIT is trained in an end-to-end manner, with the overall optimization objective defined as:

$$\mathcal{L} = \mathcal{L}_{tir} + \mathcal{L}_{cmt} + \mathcal{L}_{sdm} + \mathcal{L}_{id} \quad (7)$$

3.4. Data Augmentation

There is substantial evidence from previous research that attributes [25, 41, 54] such as color and texture play a crucial role in person retrieval tasks. The data augmentation methods we designed for the visual and textual modalities also revolve around this key aspect.

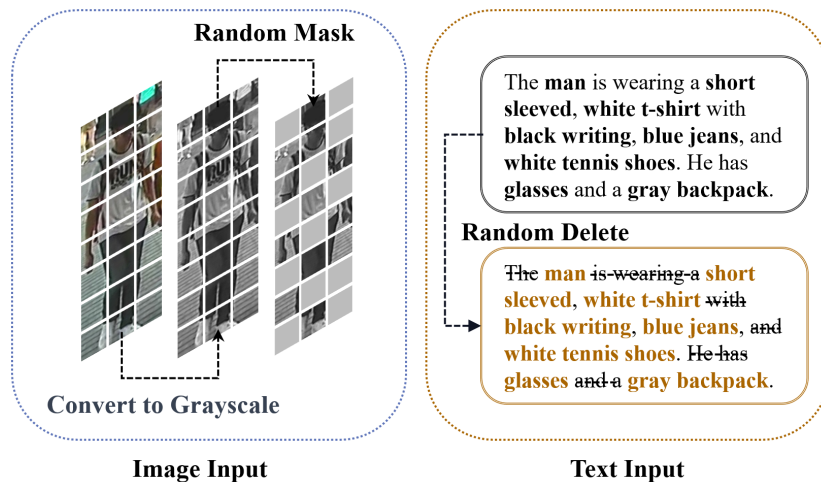


Figure 3: Illustration of data augmentation methods for the visual and textual modalities. The blue box on the left represents the conversion of image input to grayscale during the execution of the TIR auxiliary task. The grayscale image is then randomly masked and fed into the network, which is still required to recover the color image. The brown box on the right represents the deletion of non-key parts in sentences with a certain probability for text input.

3.4.1. Visual Data Augmentation

In previous studies, the auxiliary task of text-guided colorization of grayscale images was employed by LapsCore [58] to enhance the implicit alignment between color-related vocabulary in the textual modality and certain image regions in the visual modality. The effectiveness of this approach lies in the crucial importance of color information for text-to-image person retrieval tasks. For the same reasons, during the execution of the TIR auxiliary task, the images are converted to grayscale and the network is required to recover the color images. This treatment directs more attention to the color information, which is critical for person retrieval, during the implicit alignment

of text phrases and image regions, leading to improved auxiliary supervision.

3.4.2. Text Data Augmentation

In the text modality, it is desired that the network is able to recognize the key components relevant to person retrieval in the sentences and place emphasis on them. An effective cueing mechanism is needed to enable the network to quickly capture these crucial pieces of information. For text input, a method is employed where there is a small probability of preserving the attribute parts (such as pronouns, adjectives, nouns) in the sentences, and the network is trained using the processed sentences. This approach guides the network to rely more on the attribute information in the sentences for subsequent supervised tasks. As a result, when confronted with complete sentences, the network also prioritizes the utilization of attribute information.

4. Experiments

Three challenging text-to-image person retrieval datasets were employed in this study, and comprehensive evaluations were conducted. A comparison was made against state-of-the-art methods. The effectiveness of each component in our proposed framework was demonstrated through rigorous ablation study.

4.1. Datasets and Evaluation Metrics

The CUHK-PEDES dataset [40] is the first dataset dedicated to text-to-image person retrieval, comprising 40,206 images and 80,412 text descriptions, covering 13,003 identities. The training set consists of 34,054 images and 68,108 text descriptions, while the validation and test sets contain 3,078

and 3,074 images, respectively, each accompanied by 6,158 and 6,156 text descriptions. Both the validation and test sets include 1,000 identities. These images have been manually annotated, with each image having two descriptions, and the average length of all the descriptions is no less than 23 words.

The ICFG-PEDES dataset [13] consists of 54,522 images and their corresponding text descriptions, covering 4,102 identities. Each image has only one corresponding text description. The dataset is divided into a training set and a test set, with the training set containing 34,674 image-text pairs, covering 3,102 identities, and the test set containing 19,848 image-text pairs, covering 1,000 identities. Compared to CUHK-PEDES, ICFG-PEDES places more emphasis on individual identities and provides more finer-grained information in the text descriptions. The average length of the descriptions is 37 words, and the vocabulary contains 5,554 different words.

The RSTPReid dataset [65] comprises 20,505 images and 41,010 text descriptions, covering 4,101 identities. Each identity has 5 images, and each image corresponds to 2 text descriptions, with each description having a minimum length of 23 words. The dataset is captured by 15 cameras and is designed to address text-to-image person retrieval tasks in real-world scenarios. It is divided into a training set (3,701 identities), a validation set (200 identities), and a test set (200 identities).

The popular Rank-k metric is widely used to evaluate the performance of cross-modal person re-identification systems. This metric measures the probability of finding at least one matching person image within the top k candidates given a text query. Common values for k are 1, 5, and 10. A higher Rank-k score indicates that the system is more effective in returning relevant

results for the query. In addition to using the mean average precision (mAP) for evaluation, to comprehensively assess cross-modal person re-identification systems, the mean Inverse Negative Penalty [61] (mINP) is introduced as an additional evaluation criterion. The mAP considers the system’s performance on different queries by calculating the average precision of retrieved relevant images and averaging the results across all queries. On the other hand, mINP combines the ranking and relevance of image-text retrieval by calculating the inverse negative penalty for relevant image-text pairs and averaging the results across all queries. Higher values of Rank-k, mAP, and mINP indicate superior system performance.

4.2. Implementation Details

We perform our experiments on a single V100 40GB GPU. The image encoder and text encoder are initialized with pre-trained CLIP parameters, while the parameters of the TIR module are randomly initialized. For each layer of the TIR module’s decoder, the hidden feature size and the number of heads is set to 512 and 8, respectively. During the training process, in addition to the data augmentation method mentioned in section 3.4, we apply random horizontal flipping, random cropping with padding, and random erasing to the image data. The input images are resized to a width of 384 and a height of 128, with each patch size being 16×16 . The maximum length of the textual token sequence is set to 77, and there is a 0.2 probability of only retaining keywords. We utilize the Adam [30] optimizer for training, performing a total of 60 epochs with an initial learning rate of 10^{-5} . We employ cosine learning rate decay. Initially, we conduct 5 warm-up epochs, gradually increasing the learning rate from 10^{-6} linearly to 10^{-5} . For the

randomly initialized modules, the initial learning rate is set to 5×10^{-5} . The temperature parameter τ in both the CMT and SDM loss is set to 0.02. During training, the entire UIT model is trained, while during testing, only the dual-encoder structure is retained.

4.3. Comparisons with State-of-the-art Models

In this section, we present our baseline, which is the pre-trained CLIP model fine-tuned with SDM [27] loss and ID [64] loss. We compare our method with state-of-the-art approaches on three benchmark datasets as shown in Tables 1, 2, and 3. Our method demonstrates significant improvements over the baseline in all three benchmark tests and achieves state-of-the-art results.

CUHK-PEDES [40]: Firstly, we evaluate our UIT model on the most common and widely used benchmark dataset. From the results in Table 1, it can be observed that UIT achieves Rank-1, Rank-5, and Rank-10 accuracies of 75.00%, 89.98%, and 94.08% respectively, with a mAP of 67.23%. Compared to recent state-of-the-art methods, TIRA demonstrates superior performance. Additionally, we note that recent advanced methods tend to utilize Transformer structures for image-text feature extraction, while the outstanding performance of them is mostly attributed to leveraging the prior knowledge from the pre-trained CLIP model. Furthermore, the performance of our baseline model indicates that fine-tuning the pre-trained full CLIP model is a good choice. Compared to the baseline, our method achieves a 3.73% improvement in Rank-1 accuracy and a 2.21% improvement in mAP. Compared to the IRRA method, which fine-tunes the entire CLIP as well, our method exhibits significant advantages across all evaluation metrics.

Method	Type	Image Encoder	Text Encoder	Rank-1	Rank-5	Rank-10	mAP	mINP
CMPM/C[63] <small>[ECCV18]</small>	L	RN50	LSTM	49.37	-	79.27	-	-
PMA[28] <small>[AAAI20]</small>	L	RN50	LSTM	53.81	73.54	81.23	-	-
TIMAM[45] <small>[ICCV19]</small>	G	RN101	BERT	54.51	77.56	79.27	-	-
ViTAA[55] <small>[ECCV20]</small>	L	RN50	LSTM	54.92	75.18	82.90	51.60	-
NAFS[17] <small>[arXiv21]</small>	L	RN50	BERT	59.36	79.13	86.00	54.07	-
DSSL[65] <small>[MM21]</small>	L	RN50	BERT	59.98	80.41	87.56	-	-
SSAN[13] <small>[arXiv21]</small>	L	RN50	LSTM	61.37	80.15	86.73	-	-
LapsCore[58] <small>[ICCV21]</small>	L	RN50	BERT	63.40	-	87.80	-	-
ISANet[60] <small>[arXiv22]</small>	L	RN50	LSTM	63.92	82.15	87.69	-	-
LBUL[57] <small>[MM22]</small>	L	RN50	BERT	64.04	82.66	87.22	-	-
CM-MoCo[20] <small>[BMVC21]</small>	G	CLIP-RN101	CLIP-Xformer	64.08	81.73	88.19	60.08	-
SAF[38] <small>[ICASSP22]</small>	L	ViT-Base	BERT	64.13	82.62	88.40	-	-
TIPCB[10] <small>[Neuro22]</small>	L	RN50	BERT	64.26	83.19	89.10	-	-
CAIBC[56] <small>[MM22]</small>	L	RN50	BERT	64.43	82.87	88.37	-	-
AXM-Net[16] <small>[MM22]</small>	L	RN50	BERT	64.44	80.52	86.77	58.73	-
LGUR[48] <small>[MM22]</small>	L	DeiT-Small	BERT	65.25	83.12	89.00	-	-
IVT[49] <small>[ECCVW22]</small>	G	ViT-Base	BERT	65.59	83.11	89.21	-	-
CFine[59] <small>[arXiv22]</small>	L	CLIP-ViT	BERT	69.57	85.93	91.15	-	-
IRRA[27] <small>[CVPR2023]</small>	G	CLIP-ViT	CLIP-Xformer	73.38	89.93	93.71	66.13	50.24
Baseline(ViT-B)	G	CLIP-ViT	CLIP-Xformer	71.23	87.80	92.59	65.02	49.21
UIT(Ours)	G	CLIP-ViT	CLIP-Xformer	75.00	89.98	94.09	67.23	51.45

Table 1: Comparison with state-of-the-art methods on the CUHK-PEDES dataset. The results are sorted based on Rank-1 accuracy, ”-” indicates that the original paper did not use that specific metric to evaluate its models. In the ”Type” column, ”G” and ”L” represent global matching and local matching methods, respectively.

ICFG-PEDES [13]: The performance comparison on the ICFG-PEDES dataset is shown in Table 2. The baseline method achieves Rank-1, Rank-5,

Method	Type	Rank-1	Rank-5	Rank-10	mAP	mINP
Dual Path[64] <small>[TOMM20]</small>	G	38.99	59.44	68.41	-	-
CMPM/C[63] <small>[ECCV18]</small>	L	43.51	65.44	74.26	-	-
ViTAA[55] <small>[ECCV20]</small>	L	50.98	68.79	75.78	-	-
SSAN[13] <small>[arXiv21]</small>	L	54.23	72.63	79.53	-	-
TIPCB[10] <small>[Neuro22]</small>	L	54.96	74.72	81.89	-	-
IVT[49] <small>[ECCVW22]</small>	G	56.04	73.60	80.22	-	-
ISANet[60] <small>[arXiv22]</small>	L	57.73	75.42	81.72	-	-
CFine[59] <small>[arXiv22]</small>	L	60.83	76.55	82.42	-	-
IRRA[27] <small>[CVPR2023]</small>	G	63.46	80.25	85.82	38.06	7.93
Baseline(ViT-B)	G	61.07	78.32	83.91	35.96	7.14
UIT(Ours)	G	64.56	80.49	85.88	40.80	9.51

Table 2: Comparison with state-of-the-art methods on the ICFG-PEDES dataset.

and Rank-10 accuracies of 61.07%, 78.32%, and 83.91% respectively. This result demonstrates the strong performance of directly fine-tuning the pre-trained full CLIP model on this task, with performance slightly lower than the IRRA method. Compared to the baseline, our method improves Rank-1 accuracy by 3.49% and mAP by 4.84%. Compared to the recent advanced IRRA [65] method, our method achieves a 1.10% improvement in Rank-1 accuracy and a 2.74% improvement in mAP, establishing a leading advantage across all evaluation metrics. It is worth noting that the mINP metric on the ICFG-PEDES dataset is generally lower, indicating that the test set partition of this dataset poses a significant challenge for the models to find the hardest matching samples.

RSTPReid [65]: We also tested UIT on the recently released RSTPReid

Method	Type	Rank-1	Rank-5	Rank-10	mAP	mINP
DSSL[65] <small>[MM21]</small>	G	39.05	62.60	73.95	-	-
SSAN[13] <small>[arXiv21]</small>	L	43.50	67.80	77.15	-	-
LBUL[57] <small>[MM22]</small>	L	45.55	68.20	77.85	-	-
IVT[49] <small>[ECCVW22]</small>	L	46.70	70.00	78.80	-	-
CFine[59] <small>[arXiv22]</small>	L	50.55	72.50	81.60	-	-
IRRA[27] <small>[CVPR2023]</small>	G	60.20	81.30	88.20	47.17	25.28
Baseline(ViT-B)	G	58.65	80.70	87.10	46.54	24.02
UIT(Ours)	G	61.60	81.75	88.05	48.62	26.43

Table 3: Comparison with state-of-the-art methods on the RSTPReid dataset

dataset and compared the results with state-of-the-art methods, as shown in Table 3. Our method achieves a 2.95% improvement in Rank-1 accuracy and a 2.08% improvement in mAP compared to the baseline. When compared to the state-of-the-art IRRA [27] method, our method achieves a gain of 1.40% in Rank-1 accuracy and 1.45% in mAP, significantly outperforming other methods.

In conclusion, UIT consistently achieves the best performance on all three popular benchmark datasets. This demonstrates the generalization and robustness of our proposed method.

4.4. Ablation Study

In order to thoroughly demonstrate the effectiveness of each component, we conducted extensive ablation experiments using the pre-trained full CLIP model fine-tuned with SDM loss and ID loss as the baseline.

No.	Components		CUHK-PEDES			ICFG-PEDES		
	Vision	Text	Rank-1	Rank-5	Rank-10	Rank-1	Rank-5	Rank-10
1			74.76	89.69	93.81	64.32	80.32	85.64
2	✓		74.85	89.77	93.82	64.4	80.41	85.67
3		✓	74.91	89.82	94.00	64.49	80.43	85.79
4	✓	✓	75.00	89.98	94.08	64.56	80.49	85.88

Table 4: Ablation experimental results with different data augmentation techniques. "Vision" represents image-side data augmentation, "Text" represents text-side data augmentation, and "✓" indicates the usage of a particular augmentation technique.

4.4.1. The Effectiveness of Data Augmentation

In order to focus the model’s attention on information beneficial for image-text matching, we conducted targeted data augmentation on both the visual and text aspects. To thoroughly demonstrate the impact of these two data augmentation techniques, we performed related ablation experiments on two datasets (CUHK-PEDES [40] and ICFG-PEDES [13]), and the results of Rank-1, Rank-5, and Rank-10 accuracies (%) under different experimental settings are recorded in Table 4. The effectiveness of visual data augmentation is demonstrated by comparing results No. 1 to No. 2 and No. 3 to No. 4. The effectiveness of textual data augmentation is demonstrated by comparing results No. 1 to No. 3 and No. 2 to No. 4. Using each data augmentation technique individually can bring about performance improvements to some extent, but the best results are achieved when both data augmentation techniques are used together.

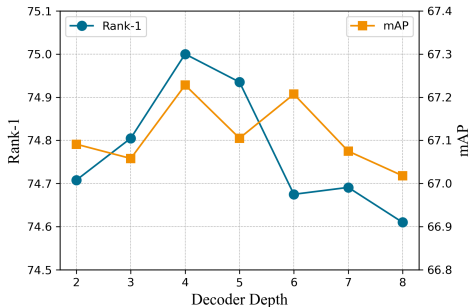
No.	Methods	Components			CUHK-PEDES			ICFG-PEDES		
		CMT	IRR	TIR	Rank-1	Rank-5	Rank-10	Rank-1	Rank-5	Rank-10
1	Baseline				71.23	87.80	92.59	61.07	78.32	83.91
2	\mathcal{L}_{cmt}	✓			71.62	87.93	92.71	61.32	78.46	84.09
3	IRR		✓		73.40	89.59	93.72	63.49	80.31	85.81
4	TIR			✓	74.71	89.73	93.89	64.27	80.33	85.85
5	\mathcal{L}_{cmt} +IRR	✓	✓		73.84	89.85	93.81	63.76	80.31	85.84
6	IRR+TIR		✓	✓	74.45	89.67	93.74	64.09	80.28	85.79
7	\mathcal{L}_{cmt} +IRR+TIR	✓	✓	✓	74.62	89.78	93.84	64.26	80.38	85.85
8	UIT	✓		✓	75.00	89.98	94.08	64.56	80.49	85.88

Table 5: Ablation experimental results on the effectiveness of each component in UIT. The "Baseline" represents the pre-trained full CLIP model fine-tuned with SDM loss and ID loss. Subsequent experimental settings utilize these two loss functions and the best data augmentation strategy.

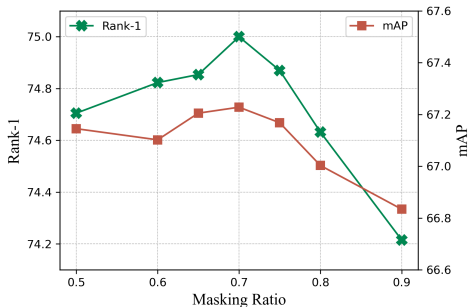
4.4.2. The Effectiveness of Proposed Components

In order to thoroughly demonstrate the impact of different components in UIT, we conducted comprehensive experiments on two datasets (CUHK-PEDES [40] and ICFG-PEDES [13]). The Rank-1, Rank-5, and Rank-10 accuracies (%) under different experimental settings are recorded in Table 5. Results No. 1 compared to No. 2, No. 3 compared to No. 5, and No. 4 compared to No. 8 demonstrate the effectiveness of our proposed components. These results indicate that adding additional supervised loss for hard samples can lead to performance improvements regardless of the specific scenario.

The TIR module facilitates fine-grained cross-modal alignment by implicitly learning the local correspondences between image patches and phrases



(a) Decoder Depth



(b) Masking Ratio

Figure 4: Ablation experiment results of the TIR module. (a) illustrates the Rank-1 and mAP metrics of UIT under different depths of the multimodal interaction decoder. (b) demonstrates the Rank-1 and mAP metrics of UIT input with varying image masking ratios when utilizing the TIR module.

through the MIM task. The effectiveness of the TIR module is demonstrated by comparing results No. 1 to No. 4 and No. 2 to No. 8. When only adding the TIR module to the baseline, the Rank-1 accuracies on both datasets are improved by 3.28% and 3.13%, respectively. Compared to the widely proven effective MLM (IRR) [27] auxiliary task, TIR still maintains advantages of 1.31% and 0.78% in Rank-1 accuracy on the two datasets.

It is worth noting that the comparison between results No. 4 and No. 6, and results No. 7 and No. 8, indicates that using two effective auxiliary tasks simultaneously does not necessarily lead to better results. In fact, it may even result in lower training efficiency and poorer performance.

4.4.3. Ablation Experiments on the TIR Module

To maximize the efficiency of our proposed multimodal interaction module, we explored the influence of the depth of it and the image masking ratio

on the performance of cross-modal person retrieval. The variations in Rank-1 accuracy and mAP under different depths of the multimodal interaction decoder are shown in Figure 4 (a). Through comparison, it is evident that a depth of 4 is the optimal choice, achieving high performance while ensuring training efficiency. The variations in Rank-1 accuracy and mAP under different image masking ratios are showed in Figure 4 (b). An image masking ratio of 0.7 is the best choice, as a very high image masking ratio (e.g., 0.9) would negatively impact the effectiveness of the module.

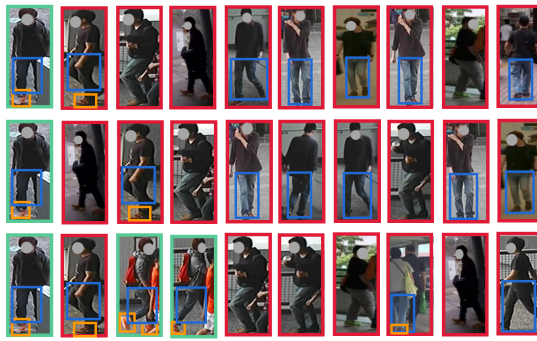
4.5. Qualitative Results

Figure 5 compares the top-10 retrieval results of the Baseline, the recently effective IRRA [27], and our proposed UIT. As shown in Figure 5, UIT achieves more accurate retrieval results and is more sensitive to person descriptions of the same identity. In most cases, even with variations in viewpoint, UIT is able to find all targets of the same identity within the top-10 retrieval results. In contrast, the Baseline and IRRA fail to demonstrate this favorable characteristic. The reason for this improvement can be attributed to two factors. Firstly, we designed the TIR module, which helps establish the correlations between text phrases and local image regions, thereby reducing the over-reliance on visual perspectives in person retrieval. Secondly, we introduced the CMT loss during the training process, which focuses more on challenging person retrieval cases and enables the network to differentiate subtle differences between individuals of different identities. This text-to-image person retrieval capability is crucial in practical applications. Furthermore, the correspondences between phrases and image patches in the figure also indicates that UIT has stronger local alignment capability.

The man is wearing a **striped collared shirt**. He is wearing black pants and black shoes. He carries a **book** and his **black coat** in his left hand.



A man wearing a black shirt, a pair of **blue jeans** and a pair of **orange shoes**.



The lady is wearing a **red mid sleeve shirt** tucked into a **light blue ruffled skirt** with **blue heels** and a **blue purse with white handles** on her right shoulder.



Figure 5: Comparison of the top 10 retrieval results between the Baseline (first row), IRRA [27] (second row), and UIT (third row) on CUHK-PEDES. Matching and non-matching images corresponding to the text description are highlighted with green and red bounding boxes, respectively. The matched textual entities and local image regions are indicated with phrases and bounding boxes of the same color in the figure.

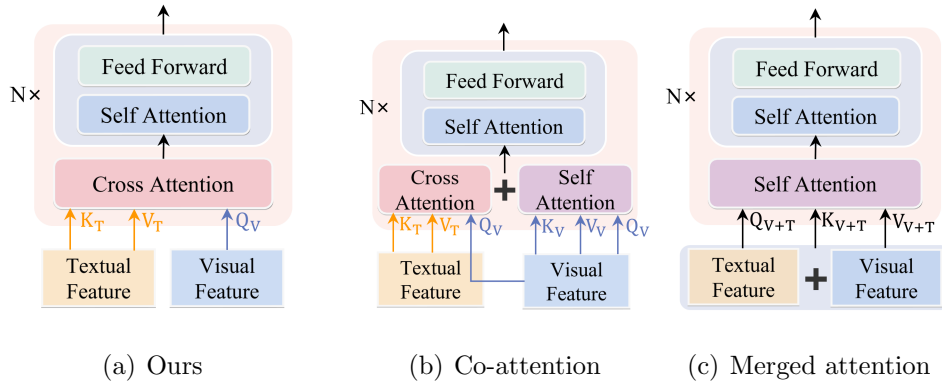


Figure 6: Illustration of different multimodal interaction decoders. (a) Our multimodal interaction encoder, where visual information is used as the query, and textual information serves as key and value for cross attention before being fed into the Transformer Block. (b) Co-attention, where visual information is used as the query, and both visual and textual information are used as key and value for separate attention before being combined and fed into the Transformer Block. (c) Merged attention, where visual and textual information are merged and then used for self-attention before being fed into the Transformer Block.

Taking the first group of images in Figure 5 as an example, the sentence contains the phrase "black coat in his left hand," and UIT finds the corresponding images in the top three retrieval results, rather than focusing separately on "black coat" and "hand."

5. Discussion

Performance in auxiliary tasks does not necessarily imply better Text-to-Image person retrieval results: Currently, incorporating auxiliary tasks into the Text-to-Image person retrieval framework has become a common practice. However, when choosing auxiliary tasks, a question arises: Does better performance in auxiliary tasks guarantee better retrieval perfor-

mance in the end? This study aims to answer this question by evaluating TIR modules with different cross-modal attention mechanisms.

Method	Rank-1	Rank-5	Rank-10
Co-Attention	74.76	89.86	93.97
Merged Attention	74.69	89.8	94.01
Ours	75.00	89.98	94.08

Table 6: Performance table of UIT using different multimodal interaction decoders. The table lists the Rank-1, Rank-5, and Rank-10 metrics of UIT with three different multimodal interaction decoders.

As shown in Figure 6, we tried three different multimodal interaction decoders and embedded them into the complete network for training and testing on the CUHK-PEDES dataset. Figure 7 presents the visualization results of the Text-guided Image Restoration, while Table 6 shows the final retrieval performance. By comparing the image restoration results of the three different multimodal interaction decoders in Figure 7, it is evident that Co-attention and Merged attention achieve better image restoration. However, the person retrieval test results in Table 6 indicate that using our current multimodal interaction encoder achieves the best retrieval performance. The reason for this could be attributed to the different multimodal interaction methods in Figure 6 (b) and Figure 6 (c). In the image restoration process, the visual information is not only used as the query but also directly involved in the restoration. While this contributes to better image restoration, it significantly weakens the dependency of the auxiliary task on text and hampers the interaction between images and texts. In contrast, our approach uses visual information as the query and textual information as



Figure 7: Illustration of image restoration results using different multimodal interaction decoders. For each set of images, from left to right, they represent the original image, the image after being masked, and the images restored by three forms of cross-attention in the multimodal interaction decoders (from left to right: Ours, Co-attention, and Merged attention).

key and value, forcing the network to utilize textual information to recover the masked image patches through cross-modal attention. Although this is a challenging task, it significantly increases the demand for interaction between texts and images, thereby achieving better retrieval performance.

In summary, having better performance in auxiliary tasks does not necessarily translate to better retrieval performance in text-to-image person retrieval. The key to improving retrieval performance lies in enhancing the interaction and connection between texts and images. By reinforcing the re-

lationship between textual and visual entities, we can achieve better results in person retrieval tasks.

6. Conclusion

Our study aims to enhance Text-to-image person retrieval performance and we also proposes a novel framework named UIT. Significant performance improvements have been achieved through the introduction of innovative methods such as the Text-guided Image Restoration auxiliary task and the Cross-Modal Triplet loss. Specifically, the Text-guided Image Restoration auxiliary task aims to recover missing image patches and establish implicit correspondences between phrases and image patches, thereby improving the retrieval accuracy of text-image embeddings. Additionally, the introduction of the Cross-Modal Triplet loss focuses on handling challenging samples, enhancing the model’s ability to differentiate minor differences. Furthermore, a novel text data augmentation method is proposed to facilitate the recognition of key components within sentences. Through these methods, the correspondences between visual and textual entities are effectively strengthened, improving the alignment of global features. The performance on three popular benchmark datasets further validates the effectiveness of the proposed UIT framework. This study further verifies the feasibility and scalability of the CLIP model with auxiliary task supervision in the field of text-to-image person retrieval. It is hoped that our work can provide inspiration for researchers in exploring other auxiliary tasks in the future.

References

- [1] Stanislaw Antol, Aishwarya Agrawal, Jiasen Lu, Margaret Mitchell, Dhruv Batra, C Lawrence Zitnick, and Devi Parikh. Vqa: Visual question answering. In *Proceedings of the IEEE international conference on computer vision*, pages 2425–2433, 2015.
- [2] Mathilde Caron, Hugo Touvron, Ishan Misra, Hervé Jégou, Julien Mairal, Piotr Bojanowski, and Armand Joulin. Emerging properties in self-supervised vision transformers. In *Proceedings of the IEEE/CVF international conference on computer vision*, pages 9650–9660, 2021.
- [3] Soravit Changpinyo, Piyush Sharma, Nan Ding, and Radu Soricut. Conceptual 12m: Pushing web-scale image-text pre-training to recognize long-tail visual concepts. In *Proceedings of the IEEE/CVF Conference on Computer Vision and Pattern Recognition*, pages 3558–3568, 2021.
- [4] Tianlang Chen, Chenliang Xu, and Jiebo Luo. Improving text-based person search by spatial matching and adaptive threshold. In *2018 IEEE Winter Conference on Applications of Computer Vision (WACV)*, pages 1879–1887. IEEE, 2018.
- [5] Xi Chen, Xiao Wang, Soravit Changpinyo, AJ Piergiovanni, Piotr Padlewski, Daniel Salz, Sebastian Goodman, Adam Grycner, Basil Mustafa, Lucas Beyer, et al. Pali: A jointly-scaled multilingual language-image model. *arXiv preprint arXiv:2209.06794*, 2022.
- [6] Xinlei Chen and Kaiming He. Exploring simple siamese representation learning. In *Proceedings of the IEEE/CVF conference on computer vision and pattern recognition*, pages 15750–15758, 2021.

- [7] Xinlei Chen, Hao Fang, Tsung-Yi Lin, Ramakrishna Vedantam, Saurabh Gupta, Piotr Dollár, and C Lawrence Zitnick. Microsoft coco captions: Data collection and evaluation server. *arXiv preprint arXiv:1504.00325*, 2015.
- [8] Xinlei Chen, Haoqi Fan, Ross Girshick, and Kaiming He. Improved baselines with momentum contrastive learning. *arXiv preprint arXiv:2003.04297*, 2020.
- [9] Yen-Chun Chen, Linjie Li, Licheng Yu, Ahmed El Kholy, Faisal Ahmed, Zhe Gan, Yu Cheng, and Jingjing Liu. Uniter: Universal image-text representation learning. In *European conference on computer vision*, pages 104–120. Springer, 2020.
- [10] Yuhao Chen, Guoqing Zhang, Yujiang Lu, Zhenxing Wang, and Yuhui Zheng. Tipcb: A simple but effective part-based convolutional baseline for text-based person search. *Neurocomputing*, 494:171–181, 2022.
- [11] Wenliang Dai, Junnan Li, Dongxu Li, Anthony Meng Huat Tiong, Junqi Zhao, Weisheng Wang, Boyang Li, Pascale Fung, and Steven Hoi. Instructblip: Towards general-purpose vision-language models with instruction tuning, 2023.
- [12] Jacob Devlin, Ming-Wei Chang, Kenton Lee, and Kristina Toutanova. Bert: Pre-training of deep bidirectional transformers for language understanding. *arXiv preprint arXiv:1810.04805*, 2018.
- [13] Zefeng Ding, Changxing Ding, Zhiyin Shao, and Dacheng Tao. Semantically self-aligned network for text-to-image part-aware person re-identification. *arXiv preprint arXiv:2107.12666*, 2021.
- [14] Alexey Dosovitskiy, Lucas Beyer, Alexander Kolesnikov, Dirk Weissenborn, Xiaohua Zhai, Thomas Unterthiner, Mostafa Dehghani, Matthias Minderer,

- Georg Heigold, Sylvain Gelly, et al. An image is worth 16x16 words: Transformers for image recognition at scale. *arXiv preprint arXiv:2010.11929*, 2020.
- [15] Zi-Yi Dou, Yichong Xu, Zhe Gan, Jianfeng Wang, Shuohang Wang, Lijuan Wang, Chenguang Zhu, Pengchuan Zhang, Lu Yuan, Nanyun Peng, et al. An empirical study of training end-to-end vision-and-language transformers. In *Proceedings of the IEEE/CVF Conference on Computer Vision and Pattern Recognition*, pages 18166–18176, 2022.
- [16] Ammarah Farooq, Muhammad Awais, Josef Kittler, and Syed Safwan Khalid. Axm-net: Implicit cross-modal feature alignment for person re-identification. In *Proceedings of the AAAI Conference on Artificial Intelligence*, volume 36, pages 4477–4485, 2022.
- [17] Chenyang Gao, Guanyu Cai, Xinyang Jiang, Feng Zheng, Jun Zhang, Yifei Gong, Pai Peng, Xiaowei Guo, and Xing Sun. Contextual non-local alignment over full-scale representation for text-based person search. *arXiv preprint arXiv:2101.03036*, 2021.
- [18] Alex Graves and Alex Graves. Long short-term memory. *Supervised sequence labelling with recurrent neural networks*, pages 37–45, 2012.
- [19] Jean-Bastien Grill, Florian Strub, Florent Altché, Corentin Tallec, Pierre Richemond, Elena Buchatskaya, Carl Doersch, Bernardo Avila Pires, Zhaohan Guo, Mohammad Gheshlaghi Azar, et al. Bootstrap your own latent—a new approach to self-supervised learning. *Advances in neural information processing systems*, 33:21271–21284, 2020.
- [20] Xiao Han, Sen He, Li Zhang, and Tao Xiang. Text-based person search with limited data. *arXiv preprint arXiv:2110.10807*, 2021.

- [21] Kaiming He, Xiangyu Zhang, Shaoqing Ren, and Jian Sun. Deep residual learning for image recognition. In *Proceedings of the IEEE conference on computer vision and pattern recognition*, pages 770–778, 2016.
- [22] Kaiming He, Ross Girshick, and Piotr Dollár. Rethinking imagenet pre-training. In *Proceedings of the IEEE/CVF International Conference on Computer Vision*, pages 4918–4927, 2019.
- [23] Kaiming He, Haoqi Fan, Yuxin Wu, Saining Xie, and Ross Girshick. Momentum contrast for unsupervised visual representation learning. In *Proceedings of the IEEE/CVF conference on computer vision and pattern recognition*, pages 9729–9738, 2020.
- [24] Kaiming He, Xinlei Chen, Saining Xie, Yanghao Li, Piotr Dollár, and Ross Girshick. Masked autoencoders are scalable vision learners. In *Proceedings of the IEEE/CVF conference on computer vision and pattern recognition*, pages 16000–16009, 2022.
- [25] Shuting He, Hao Luo, Pichao Wang, Fan Wang, Hao Li, and Wei Jiang. Transreid: Transformer-based object re-identification. In *Proceedings of the IEEE/CVF international conference on computer vision*, pages 15013–15022, 2021.
- [26] Chao Jia, Yinfei Yang, Ye Xia, Yi-Ting Chen, Zarana Parekh, Hieu Pham, Quoc Le, Yun-Hsuan Sung, Zhen Li, and Tom Duerig. Scaling up visual and vision-language representation learning with noisy text supervision. In *International conference on machine learning*, pages 4904–4916. PMLR, 2021.
- [27] Ding Jiang and Mang Ye. Cross-modal implicit relation reasoning and aligning

- for text-to-image person retrieval. In *Proceedings of the IEEE/CVF Conference on Computer Vision and Pattern Recognition*, pages 2787–2797, 2023.
- [28] Ya Jing, Chenyang Si, Junbo Wang, Wei Wang, Liang Wang, and Tieniu Tan. Pose-guided multi-granularity attention network for text-based person search. In *Proceedings of the AAAI Conference on Artificial Intelligence*, volume 34, pages 11189–11196, 2020.
- [29] Wonjae Kim, Bokyung Son, and Ildoo Kim. Vilt: Vision-and-language transformer without convolution or region supervision. In *International Conference on Machine Learning*, pages 5583–5594. PMLR, 2021.
- [30] Diederik P. Kingma and Jimmy Ba. Adam: A method for stochastic optimization. *arXiv: Learning, arXiv: Learning*, Dec 2014.
- [31] Ryan Kiros, Ruslan Salakhutdinov, and Richard S Zemel. Unifying visual-semantic embeddings with multimodal neural language models. *arXiv preprint arXiv:1411.2539*, 2014.
- [32] Ranjay Krishna, Yuke Zhu, Oliver Groth, Justin Johnson, Kenji Hata, Joshua Kravitz, Stephanie Chen, Yannis Kalantidis, Li-Jia Li, David A Shamma, et al. Visual genome: Connecting language and vision using crowdsourced dense image annotations. *International journal of computer vision*, 123:32–73, 2017.
- [33] Alex Krizhevsky, Ilya Sutskever, and Geoffrey E Hinton. Imagenet classification with deep convolutional neural networks. *Advances in neural information processing systems*, 25, 2012.
- [34] Jie Lei, Xinlei Chen, Ning Zhang, Mengjiao Wang, Mohit Bansal, Tamara L

- Berg, and Licheng Yu. Loopitr: Combining dual and cross encoder architectures for image-text retrieval. *arXiv preprint arXiv:2203.05465*, 2022.
- [35] Junnan Li, Ramprasaath Selvaraju, Akhilesh Gotmare, Shafiq Joty, Caiming Xiong, and Steven Chu Hong Hoi. Align before fuse: Vision and language representation learning with momentum distillation. *Advances in neural information processing systems*, 34:9694–9705, 2021.
- [36] Junnan Li, Dongxu Li, Caiming Xiong, and Steven Hoi. Blip: Bootstrapping language-image pre-training for unified vision-language understanding and generation. In *International Conference on Machine Learning*, pages 12888–12900. PMLR, 2022.
- [37] Junnan Li, Dongxu Li, Silvio Savarese, and Steven Hoi. Blip-2: Bootstrapping language-image pre-training with frozen image encoders and large language models. *arXiv preprint arXiv:2301.12597*, 2023.
- [38] Shiping Li, Min Cao, and Min Zhang. Learning semantic-aligned feature representation for text-based person search. In *ICASSP 2022-2022 IEEE International Conference on Acoustics, Speech and Signal Processing (ICASSP)*, pages 2724–2728. IEEE, 2022.
- [39] Shuang Li, Tong Xiao, Hongsheng Li, Wei Yang, and Xiaogang Wang. Identity-aware textual-visual matching with latent co-attention. In *Proceedings of the IEEE International Conference on Computer Vision*, pages 1890–1899, 2017.
- [40] Shuang Li, Tong Xiao, Hongsheng Li, Bolei Zhou, Dayu Yue, and Xiaogang Wang. Person search with natural language description. In *Proceedings of*

- the *IEEE conference on computer vision and pattern recognition*, pages 1970–1979, 2017.
- [41] Hao Luo, Youzhi Gu, Xingyu Liao, Shenqi Lai, and Wei Jiang. Bag of tricks and a strong baseline for deep person re-identification. In *Proceedings of the IEEE/CVF conference on computer vision and pattern recognition workshops*, pages 0–0, 2019.
- [42] Antoine Miech, Jean-Baptiste Alayrac, Ivan Laptev, Josef Sivic, and Andrew Zisserman. Thinking fast and slow: Efficient text-to-visual retrieval with transformers. In *Proceedings of the IEEE/CVF Conference on Computer Vision and Pattern Recognition*, pages 9826–9836, 2021.
- [43] Vicente Ordonez, Girish Kulkarni, and Tamara Berg. Im2text: Describing images using 1 million captioned photographs. *Advances in neural information processing systems*, 24, 2011.
- [44] Alec Radford, Jong Wook Kim, Chris Hallacy, Aditya Ramesh, Gabriel Goh, Sandhini Agarwal, Girish Sastry, Amanda Askell, Pamela Mishkin, Jack Clark, et al. Learning transferable visual models from natural language supervision. In *International conference on machine learning*, pages 8748–8763. PMLR, 2021.
- [45] Nikolaos Sarafianos, Xiang Xu, and Ioannis A Kakadiaris. Adversarial representation learning for text-to-image matching. In *Proceedings of the IEEE/CVF international conference on computer vision*, pages 5814–5824, 2019.
- [46] Christoph Schuhmann, Richard Vencu, Romain Beaumont, Robert Kaczmarczyk, Clayton Mullis, Aarush Katta, Theo Coombes, Jenia Jitsev, and Aran

- Komatsuzaki. Laion-400m: Open dataset of clip-filtered 400 million image-text pairs. *arXiv preprint arXiv:2111.02114*, 2021.
- [47] Rico Sennrich, Barry Haddow, and Alexandra Birch. Neural machine translation of rare words with subword units. *arXiv preprint arXiv:1508.07909*, 2015.
- [48] Zhiyin Shao, Xinyu Zhang, Meng Fang, Zhifeng Lin, Jian Wang, and Changxing Ding. Learning granularity-unified representations for text-to-image person re-identification. In *Proceedings of the 30th ACM International Conference on Multimedia*, pages 5566–5574, 2022.
- [49] Xiujun Shu, Wei Wen, Haoqian Wu, Keyu Chen, Yiran Song, Ruizhi Qiao, Bo Ren, and Xiao Wang. See finer, see more: Implicit modality alignment for text-based person retrieval. In *European Conference on Computer Vision*, pages 624–641. Springer, 2022.
- [50] Karen Simonyan and Andrew Zisserman. Very deep convolutional networks for large-scale image recognition. *arXiv preprint arXiv:1409.1556*, 2014.
- [51] Weijie Su, Xizhou Zhu, Yue Cao, Bin Li, Lewei Lu, Furu Wei, and Jifeng Dai. Vi-bert: Pre-training of generic visual-linguistic representations. *arXiv preprint arXiv:1908.08530*, 2019.
- [52] Siqu Sun, Yen-Chun Chen, Linjie Li, Shuohang Wang, Yuwei Fang, and Jingjing Liu. Lightningdot: Pre-training visual-semantic embeddings for real-time image-text retrieval. In *Proceedings of the 2021 Conference of the North American Chapter of the Association for Computational Linguistics: Human Language Technologies*, pages 982–997, 2021.

- [53] Ashish Vaswani, Noam Shazeer, Niki Parmar, Jakob Uszkoreit, Llion Jones, Aidan N Gomez, Łukasz Kaiser, and Illia Polosukhin. Attention is all you need. *Advances in neural information processing systems*, 30, 2017.
- [54] Haochen Wang, Jiayi Shen, Yongtuo Liu, Yan Gao, and Efstratios Gavves. Nformer: Robust person re-identification with neighbor transformer. In *Proceedings of the IEEE/CVF Conference on Computer Vision and Pattern Recognition*, pages 7297–7307, 2022.
- [55] Zhe Wang, Zhiyuan Fang, Jun Wang, and Yezhou Yang. Vitaa: Visual-textual attributes alignment in person search by natural language. In *Computer Vision—ECCV 2020: 16th European Conference, Glasgow, UK, August 23–28, 2020, Proceedings, Part XII 16*, pages 402–420. Springer, 2020.
- [56] Zijie Wang, Aichun Zhu, Jingyi Xue, Xili Wan, Chao Liu, Tian Wang, and Yifeng Li. Caibc: Capturing all-round information beyond color for text-based person retrieval. In *Proceedings of the 30th ACM International Conference on Multimedia*, pages 5314–5322, 2022.
- [57] Zijie Wang, Aichun Zhu, Jingyi Xue, Xili Wan, Chao Liu, Tian Wang, and Yifeng Li. Look before you leap: Improving text-based person retrieval by learning a consistent cross-modal common manifold. In *Proceedings of the 30th ACM International Conference on Multimedia*, pages 1984–1992, 2022.
- [58] Yushuang Wu, Zizheng Yan, Xiaoguang Han, Guanbin Li, Changqing Zou, and Shuguang Cui. Lapscore: language-guided person search via color reasoning. In *Proceedings of the IEEE/CVF International Conference on Computer Vision*, pages 1624–1633, 2021.
- [59] Shuanglin Yan, Neng Dong, Liyan Zhang, and Jinhui Tang. Clip-driven fine-

- grained text-image person re-identification. *arXiv preprint arXiv:2210.10276*, 2022.
- [60] Shuanglin Yan, Hao Tang, Liyan Zhang, and Jinhui Tang. Image-specific information suppression and implicit local alignment for text-based person search. *arXiv preprint arXiv:2208.14365*, 2022.
- [61] Mang Ye, Jianbing Shen, Gaojie Lin, Tao Xiang, Ling Shao, and Steven C. H. Hoi. Deep learning for person re-identification: A survey and outlook. *IEEE Transactions on Pattern Analysis and Machine Intelligence*, page 2872–2893, Jun 2022. doi: 10.1109/tpami.2021.3054775. URL <http://dx.doi.org/10.1109/tpami.2021.3054775>.
- [62] Jiahui Yu, Zirui Wang, Vijay Vasudevan, Legg Yeung, Mojtaba Seyedhosseini, and Yonghui Wu. Coca: Contrastive captioners are image-text foundation models. *arXiv preprint arXiv:2205.01917*, 2022.
- [63] Ying Zhang and Huchuan Lu. Deep cross-modal projection learning for image-text matching. In *Proceedings of the European conference on computer vision (ECCV)*, pages 686–701, 2018.
- [64] Zhedong Zheng, Liang Zheng, Michael Garrett, Yi Yang, Mingliang Xu, and Yi-Dong Shen. Dual-path convolutional image-text embeddings with instance loss. *ACM Transactions on Multimedia Computing, Communications, and Applications (TOMM)*, 16(2):1–23, 2020.
- [65] Aichun Zhu, Zijie Wang, Yifeng Li, Xili Wan, Jing Jin, Tian Wang, Fangqiang Hu, and Gang Hua. Dssl: Deep surroundings-person separation learning for text-based person retrieval. In *Proceedings of the 29th ACM International Conference on Multimedia*, pages 209–217, 2021.